Quantitative Analysis of Packing Heterogeneity and Its Influence on Band Broadening in HPLC Columns

Philipps Universität Marburg
MAX-PLANCK-GESELLSCHAFT

Siarhei Khirevich[1], **Alexandra Höltzel**[1], **Anton Daneyko**[1], **Andreas Seidel-Morgenstern**[2] **and Ulrich Tallarek**[1]

[1]Department of Chemistry, Philipps-Universität Marburg, Hans-Meerwein-Strasse, 35032 Marburg, Germany
E-mail: khirevich@gmail.com, tallarek@staff.uni-marburg.de
[2]Max Planck Institute for Dynamics of Complex Technical Systems, Sandtorstrasse 1, 39106 Magdeburg, Germany

Introduction

An adequate quantification of the actual disorder or microstructural degree of heterogeneity of all the different possible HPLC packings, even at the same packing density, preferably in a strong and sensitive correlation to the experimentally observable hydrodynamic dispersion (band broadening), has not yet been demonstrated. Commonly, packing microstructures are referenced as more homogeneous or more heterogeneous. These qualitative terms may be intuitive and are most likely based on the column performance; however, they do not allow for a sound scientific quantification of the degree of heterogeneity of the underlying (very individual) packing microstructure. In this study,[1] we correlate hydrodynamic dispersion in three-dimensional bulk random packings of spherical particles with a scalar geometrical measure, which sensitively captures the microstructural heterogeneity of the packings.

Our numerical approach is implemented by in-house developed program codes and includes three consecutive steps: generation of random-close sphere packings, use of the lattice-Boltzmann method (LBM) for simulation of low-Reynolds number flow within the interparticle void space, and simulation of mass transport involving the random-walk particle-tracking method (RWPT). The last two numerical approaches are alternatives compared to the traditional Eulerian methods. The local update rule of both LBM and RWPT enables effective parallelization of the programs, and allowed us to use one of the fastest supercomputers up to date — JUGENE in Jülich (Germany). Exceptional computational facilities and appropriate numerical methods made it possible to perform about 7000 simulations of mass transport in random sphere packings and to correlate transport processes in the interparticle void space with geometrical properties of the packings.

Random packing generation

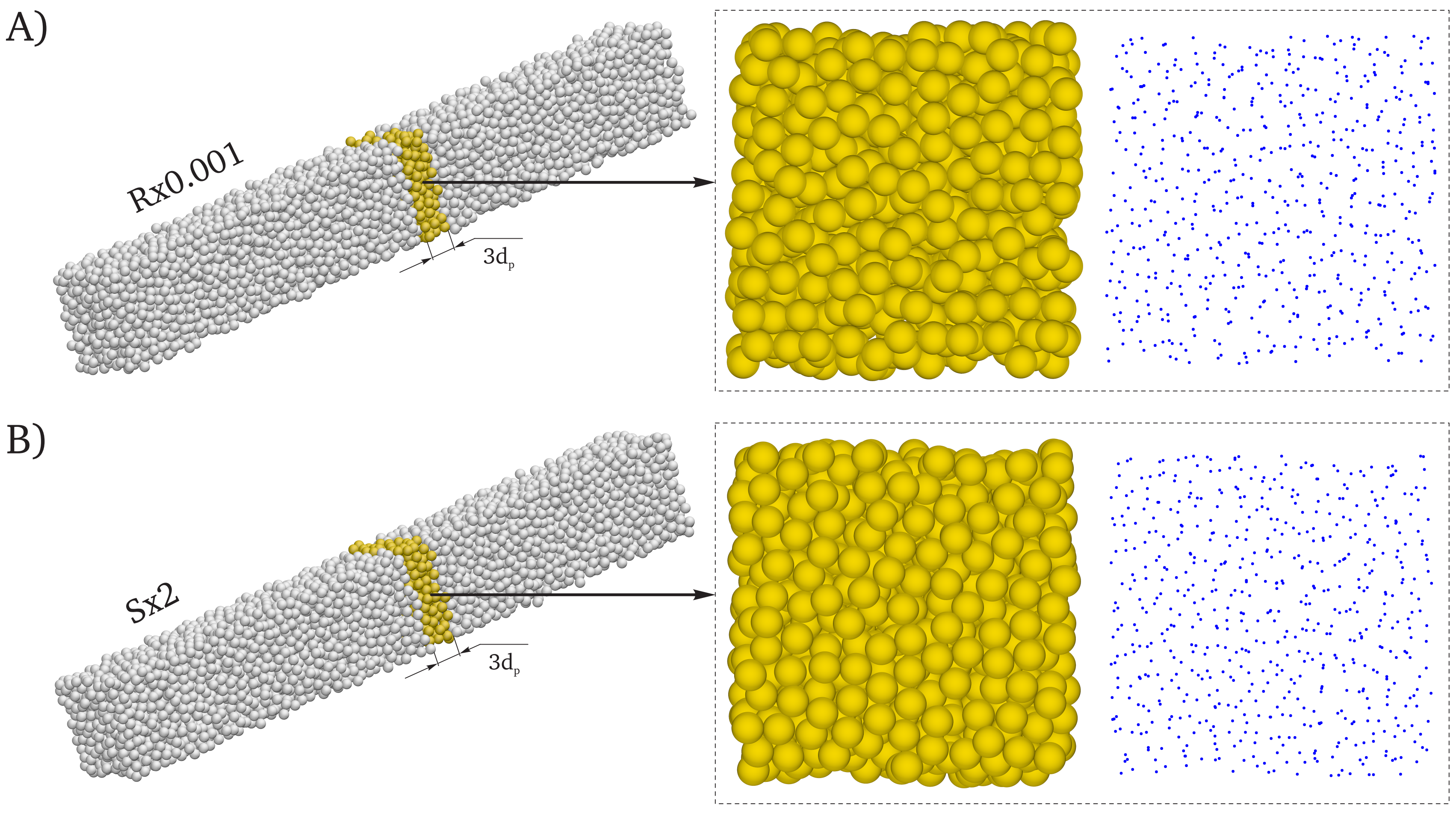

Figure 1. Unconfined random sphere packings at the random-loose packing limit ($\varepsilon = 0.46$) of two types Rx0.001 (A) and Sx2 (B). Shown are packing side views (left), sections of three particle layers as a front view (center) and corresponding projections of particle centers onto the front plane (right). Differences between the two packing types are not discernible. Therefore, we use 2D disks to illustrate the differences between packing types (Fig. 2).

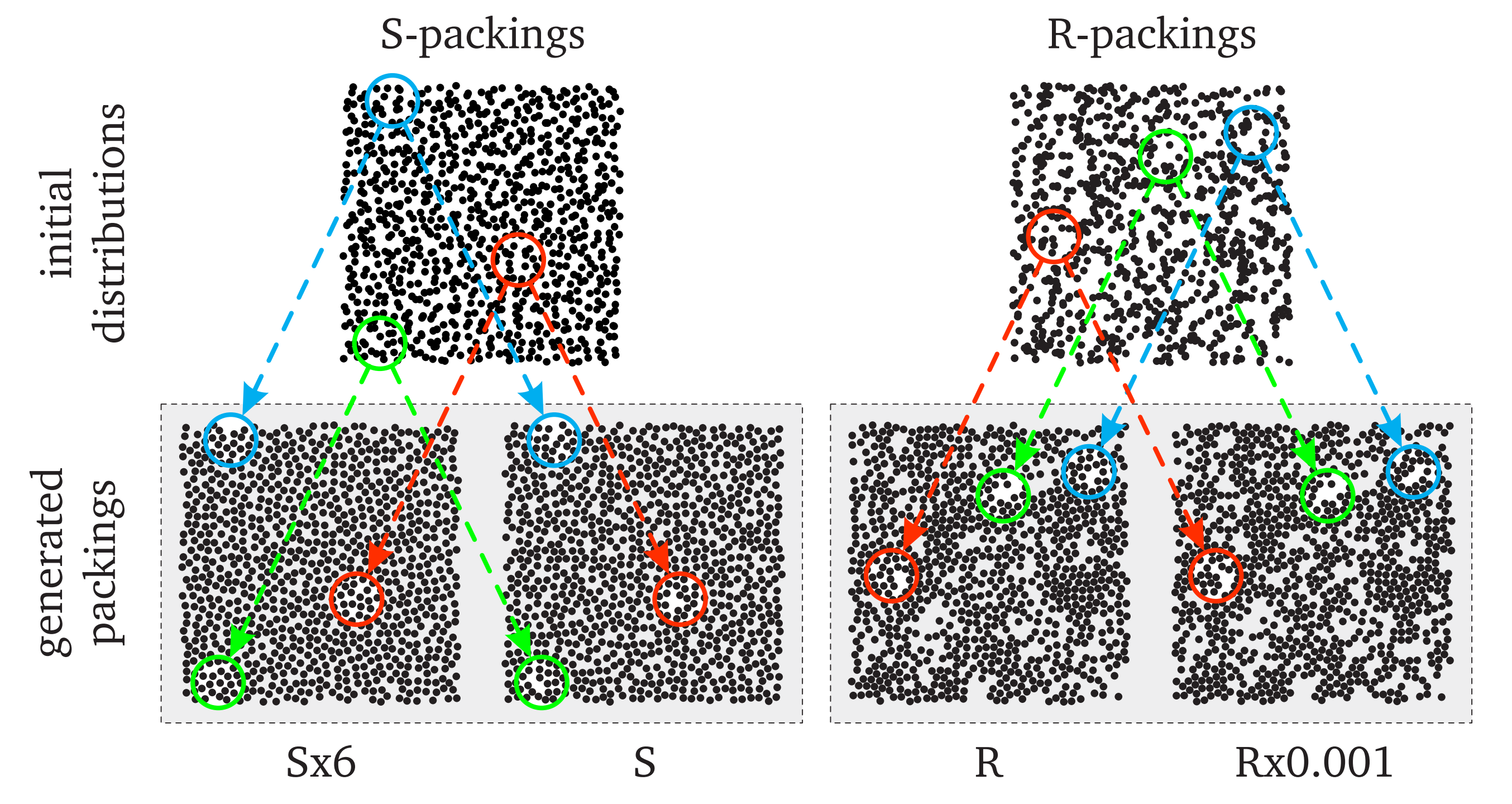

Figure 2. Unconfined random packings of monosized hard disks at $\varepsilon = 0.46$ generated with different packing protocols. Here disks are used instead of spheres for better illustration of the differences between different packing types. Generated packings are referred as "TxM," where "T" is the initial distribution type and "M" is the magnitude of displacement (see main text). In case of M = 1, packings are referred to as just "T." For example, Sx2 denotes a packing of S-type generated with magnitude of displacement 2. The figure shows the initial distributions of the disks for S- and R-types (top) and the generated 2D packings (Sx6, S, R, Rx0.001; bottom). R-packings originate from a random uniform initial distribution of disk centers in the simulation box. To generate S-packings, the simulation box was initially divided into n equal cubic cells (n is the amount of particles) and each disk center was then placed in a random position into a cell. Both types of initial distributions result in a uniform random distribution of particle centers within the simulation box. With a small magnitude of displacement the particle centers tend to stay closer to their initial positions so that the final configuration reflects the randomness of the initial distribution. A larger displacement value provides a more uniform final distribution of particle centers. Circles drawn around several regions help to compare the microstructure in the initial distributions with that of the final packings.

Isotropic random monosized hard-sphere packings with periodic boundary conditions and dimensions of $10d_p \times 10d_p \times 70d_p$ (d_p is the sphere diameter) were generated using a modified Jodrey-Tory (JT) algorithm.[2] The dimensions of packing are sufficient for performing both statistical analysis of packing microstructure and simulations of hydrodynamic dispersion within the void space of a packing. JT algorithm distributes randomly particle centers in simulation domain and iteratively removes overlaps between spheres by spreading apart of two closest sphere centers on each iteration. The initial random arrangement of sphere centers, the magnitude of closest pair displacement, and packing porosity (void space fraction) define the *degree of heterogeneity* (DoH) of final packing microstructure (Figure 2).

Statistical analysis of packings and simulation of fluid flow

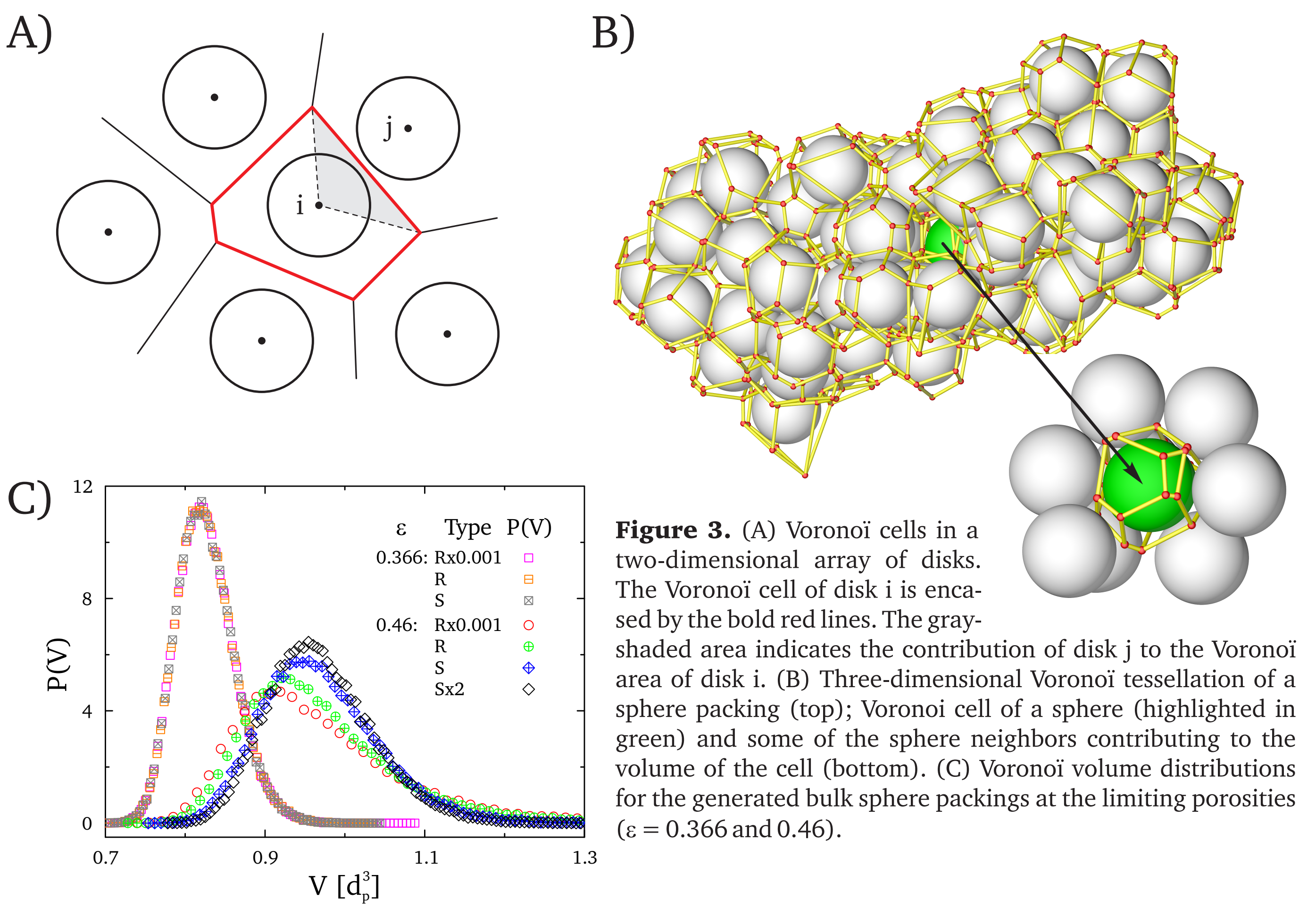

Figure 3. (A) Voronoï cells in a two-dimensional array of disks. The Voronoï cell of disk i is encased by the bold red lines. The gray-shaded area indicates the contribution of disk j to the Voronoï area of disk i. (B) Three-dimensional Voronoï tessellation of a sphere packing (top); Voronoi cell of a sphere (highlighted in green) and some of the sphere neighbors contributing to the volume of the cell (bottom). (C) Voronoï volume distributions for the generated bulk sphere packings at the limiting porosities ($\varepsilon = 0.366$ and 0.46).

A sensitive analysis tool for probing the local packing density and disorder in packed beds is the determination of Voronoï cells.[3] A Voronoï cell is the generalization of a Wigner-Seitz cell for disordered structures. For a packing of monosized spheres it is the polyhedron that contains all points closer to a given sphere center than to any other (Fig. 3A, B). Voronoï tessellation partitions the whole space of a sphere packing into a set of non-overlapping Voronoï volumes V, which are inherently associated with the local packing density. The packing is represented quantitatively by the Voronoï volume distribution P(V) (Fig. 3C). We used the Quickhull algorithm[4] to compute the volume V of the Voronoï cells.

Figure 4. Statistical analysis of the Voronoï volume distributions P(V) for the bulk sphere packings. (A) Standard deviation and (B) skewness as a function of packing type (Rx0.001, R, S, Sx2) and porosity ($0.366 \leqslant \varepsilon \leqslant 0.46$). Error bars indicate upper and lower bounds of 95% confidence intervals. (C) Profiles of the fluid flow velocity field for most heterogeneous (Rx0.001, $\varepsilon = 0.46$) and one of the most homogeneous (R, $\varepsilon = 0.366$) generated packings.

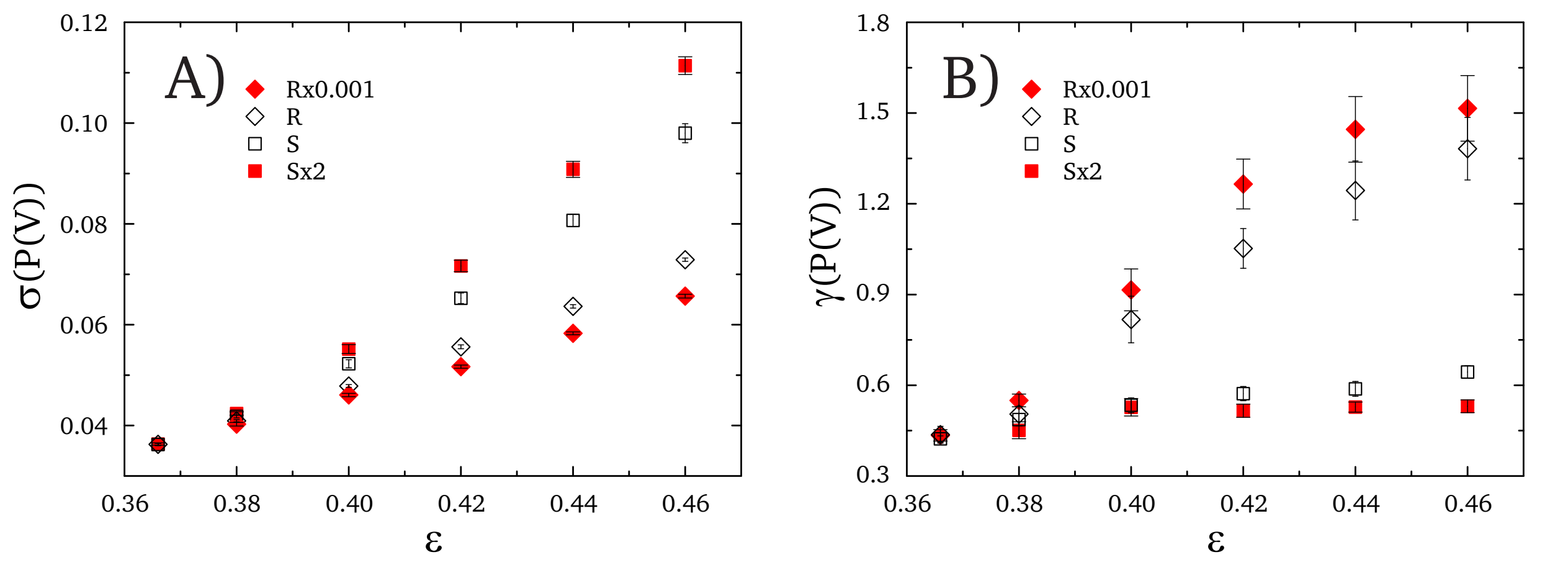

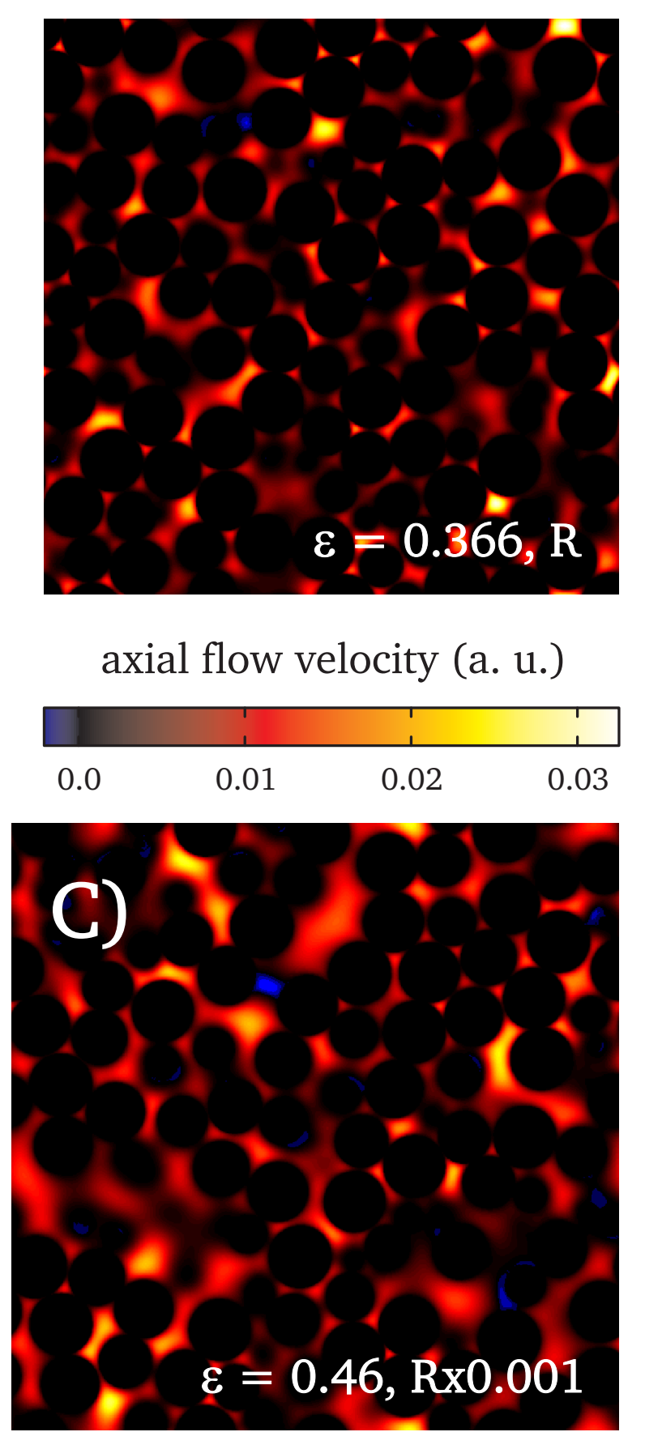

Simulation of mass transport

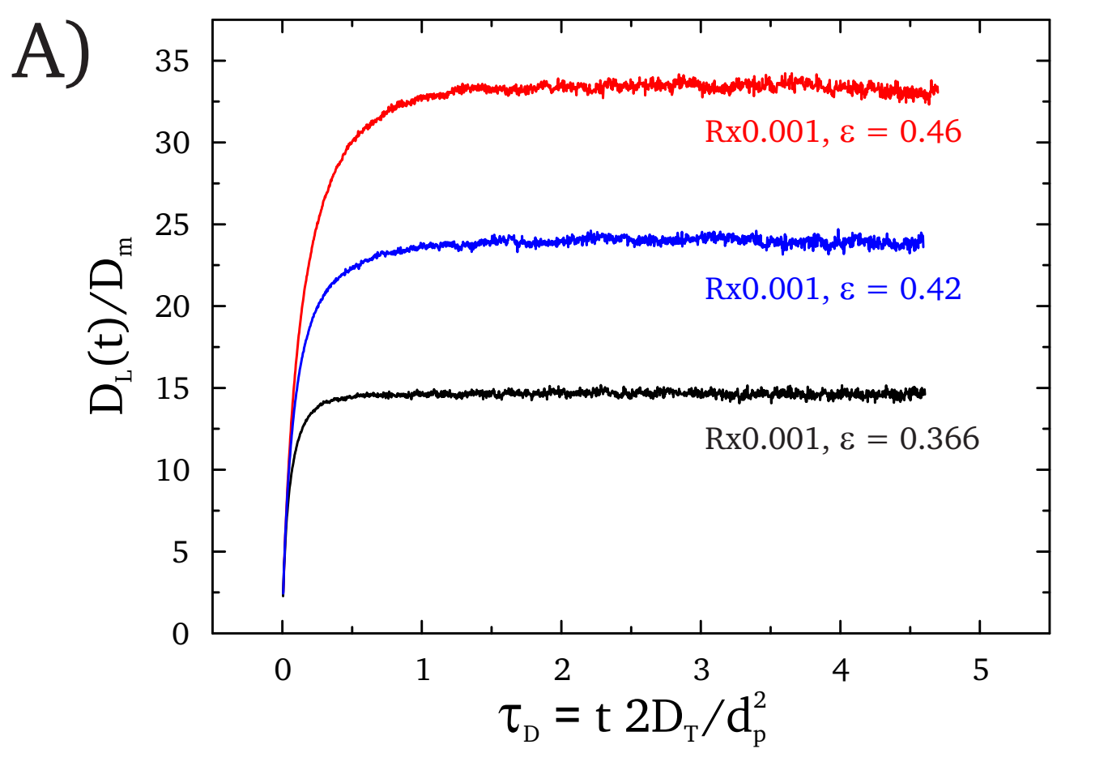

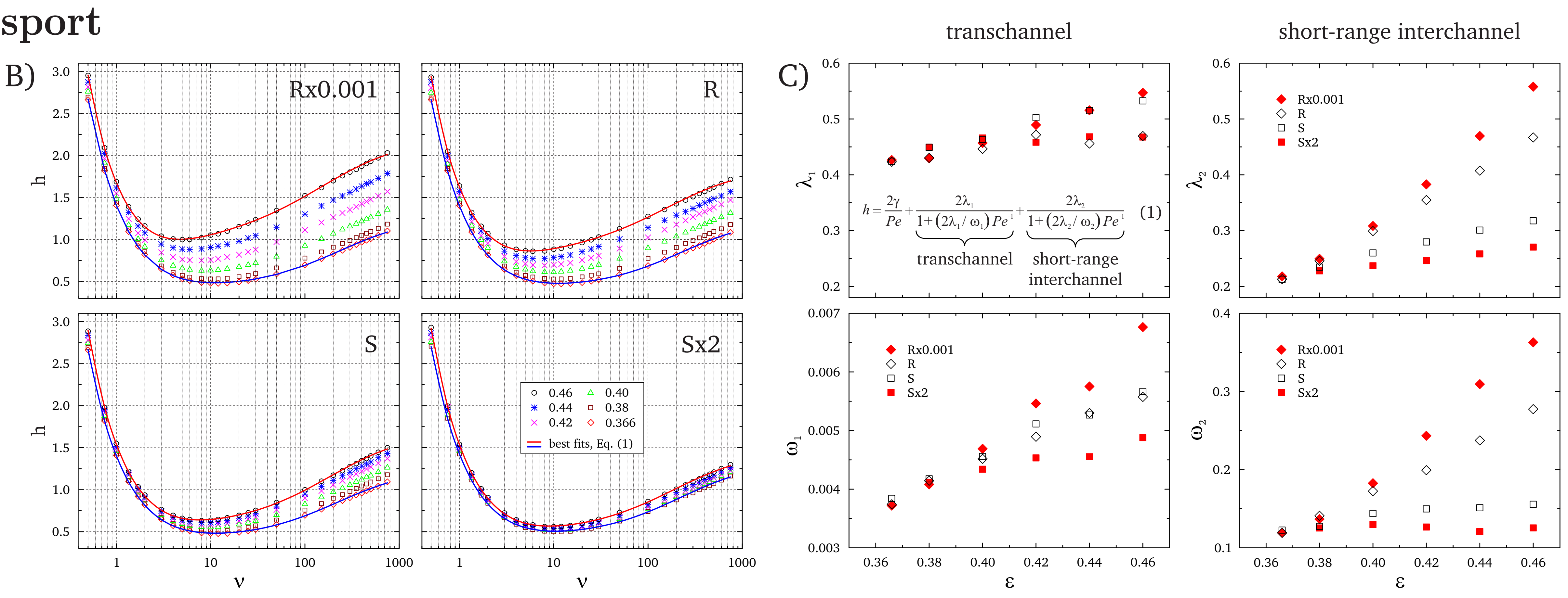

$$h = \frac{2\gamma}{Pe} + \underbrace{\frac{2\lambda_1}{1 + (2\lambda_1/\omega_1)\,Pe^{-1}}}_{\text{transchannel}} + \underbrace{\frac{2\lambda_2}{1 + (2\lambda_2/\omega_2)\,Pe^{-1}}}_{\text{short-range interchannel}} \quad (1)$$

Figure 5. (A) Shown is the time evolution of normalized longitudinal dispersion coefficients $D_L(t)/D_m$ at $\nu = u_{av}d_p/D_m = 50$ for Rx0.001 packings at porosities of $\varepsilon = 0.366$, 0.42, and 0.46. Analysis of transient dispersion in the bulk sphere packings reveals two length-scales of eddy disperison[5] in bulk packings: a short-range interchannel contribution on the single-particle scale (1–1.5 d_p) and the trans-channel contribution, which naturally exists in any packed bed on the scale of an individual channel between the particles ($\ll d_p$).
(B) Dependence of the reduced plate height $h = H/d_p$ on the reduced velocity ν ($0.5 \leqslant \nu \leqslant 750$) and the porosity ε ($0.366 \leqslant \varepsilon \leqslant 0.46$) for the four different types of bulk packings (Rx0.001, R, S, Sx2). Each value of h represents the average from ten generated packings. Solid lines are the best fits of the data at $\varepsilon = 0.366$ and 0.46 to Eq. (1).
(C) Dependence of the parameters for the transchannel contribution (λ_1 and ω_1; left column) and the short-range interchannel contribution (λ_2 and ω_2; right column) on packing protocol and porosity. Values were obtained from the best fits of the comprehensive data set of Fig. 5B to the condensed Giddings equation for bulk packings, Eq. (1).

Conclusion

Statistical analysis of packed beds by the standard deviation and skewness of the Voronoï volume distributions (Figs. 3C and 4) provides quantitative scalar measures for local disorder in packing microstructure that correlate strongly with the resulting eddy dispersion. Therefore, the presented approach defines a straight route to quantitative structure-transport relationships. Transport phenomena relevant to chromatography can be analyzed in detail by direct numerical simulations and correlated, e.g., with the generalized Giddings equation. Complementary analysis of the transient dispersion domain allows to identify the spatial scales of disorder in the packings, which helps to condense the number of scales of velocity disparity in a packing proposed by Giddings.[6] In the investigated bulk packings, we identified only the transchannel and a short-range interchannel effect to contribute to eddy dispersion (Fig. 5A). This result is in excellent agreement with our statistical analysis based on the Voronoï volume distributions, which revealed a packing porosity and protocol-dependent short-range disorder, in a strong correlation with the short-range interchannel contribution to eddy dispersion (Figs. 4 and 5C).

Acknowledgments

Computational resources on IBM BlueGene/P platforms were provided by "Genius" at RZG (Rechenzentrum Garching, Germany) and "Jugene" at FZJ (Forschungszentrum Jülich, Germany). We thank the DEISA Consortium (www.deisa.eu), co-funded through the EU FP6 project RI-031513 and the FP7 project RI-222919, for support within the DEISA Extreme Computing Initiative.

References

(1)Khirevich, S.; Daneyko, A.; Höltzel, A.; Seidel-Morgenstern, A.; Tallarek, U. *Statistical analysis of packed beds, the origin of short-range disorder, and its impact on eddy dispersion.* J. Chromatogr. A, 28: 4713, **2010**
(2)Jodrey, W. S.; Tory, E. M. *Computer simulation of close random packing of equal spheres.* Phys. Rev. A, 32: 2347, **1985**
(3)Okabe, A.; Boots, B.; Sugihara, K.; Chiu, S. N. *Spatial tessellations: concepts and applications of Voronoï diagrams.* John Wiley & Sons Ltd.: Chichester, England, **2000**
(4)Barber, C. B.; Dobkin, D. P.; Huhdanpaa, H. *The quickhull algorithm for convex hulls.* ACM Trans. Math. Softw., 22: 469, **1996**
(5)Khirevich, S.; Höltzel, A.; Seidel-Morgenstern, A.; Tallarek, U. *Time and length scales of eddy dispersion in chromatographic beds*. Anal. Chem., 81: 7057, **2009**
(6)Giddings, J. C. *Dynamics of Chromatography, Part 1: Principles and Theory*; Marcel Dekker: New York, **1965**